Orientation effects in charge exchange: Probing short-range repulsion by interference patterns

A. K. Kazansky and V. N. Ostrovsky
Institute of Physics, The University of St. Petersburg, 198904 St. Petersburg, Russia
(Received 18 February 1994)

The orientation created in the charge-exchange process $B^{3+}+He \rightarrow B^{2+}(2p)+He^{+}$ is considered, emphasizing the problem of the formation of the angular distribution in the final state. The interfering contributions to the orientation parameter are generated by the trajectories corresponding to the same scattering angle but differing by the impact parameters. Such trajectories exist only when the short-range repulsion on the initial diabatic potential curve is taken into account. Thus, the orientation effects probe the core of the atom-atom interaction in the initial state.

PACS number(s): 34.70.+e, 34.50.Pi

I. INTRODUCTION

The effects related to electron orbital asymmetry can be observed in a wide scope of collision processes [1,2]. In particular, the orbital asymmetry effects in charge exchange have recently attracted much attention both in theory and experiment (for a review see, e.g., Refs. [3,4]).

The simplest process is represented by the charge exchange between the atomic s and p states. One of the three p substates is not coupled with the others (namely, the p state orthogonal to the collision plane). Hence, at least three states are involved in the process: the active electron s state on one of the collision partners and two p substates on the other center. For small collision velocities the quasimolecular description is applicable and the minimal basis should include three molecular states correlated with the aforementioned atomic states. The physical features of the process are governed by the coupling between these states which could be described by various models.

The charge-exchange process

$$B^{3+}+He \rightarrow B^{2+}(2p)+He^{+} \tag{1.1}$$

observed by Roncin *et al.* [5] represents one of the simplest feasible cases since a well-manifested Landau-Zener pseudocrossing between the initial and final quasimolecular Σ curves occurs at quite large internuclear separations $R=R_c=7.4a_0$. Figure 1 shows the *diabatic* potential curves used in the calculations below; they cross at $R=R_c$. Thus, the charge-exchange transitions from the initial quasimolecular state Σ_i (in the entrance channel) to the $2p\sigma\Sigma$ state (in the exit channel) are well localized at the internuclear separations $R \approx R_c$. These transitions are induced by the radial motion of the atomic nuclei.

The final $2p$ states are also correlated with the $2p\pi\Pi_+$ potential curve (symmetrical under reflection in the collision plane) which at large R is quasidegenerate with the $2p\sigma\Sigma$ curve (Fig. 1). The coupling between the Σ_i and $2p\pi\Pi_+$ states is induced by the internuclear axis rotation. As shown by Ostrovsky [6,7], the rotation-induced charge exchange is negligible for small collision velocities typical in the experiments [5] ($v \approx 0.07$ a.u. for the incident ion energy 1.5 keV). However, the coupling between the exit $2p\sigma\Sigma$ and $2p\pi\Pi_+$ channels is crucial for the understanding of the electron orbital orientation in the final $2p$ state. This coupling does not lead to the charge exchange but mixes the final p substates. Its effect can be described as one-center depolarizing transitions.

A transparent physical explanation of the mechanism creating the final-state orientation was put forward recently [6] (similar ideas had also been suggested by Jaecks *et al.* [8] and Eriksen *et al.* [9]). The basic point is that the coupling between the quasimolecular $2p\sigma\Sigma$ and $2p\pi\Pi_+$ states is very strong due to their quasidegeneracy at large R. The simplest picture is obtained in the space-

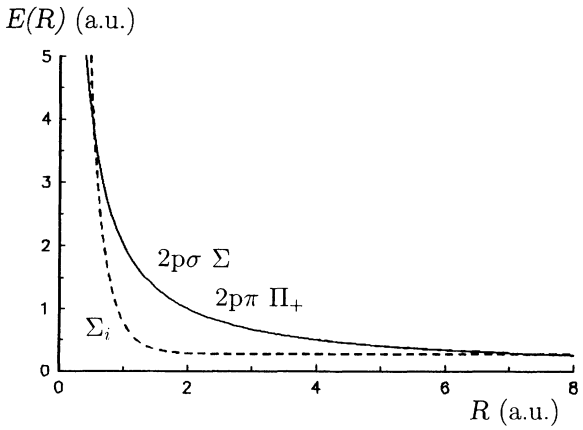

FIG. 1. The diabatic potential curves $E(R)$ used in the interpretation of the orientation effects in the process $B^{3+}+He \rightarrow B^{2+}(2p)+He^{+}$. Only the region of intermediate internuclear distances R is shown. The solid curve presents quasidegenerate $2p\sigma\Sigma$ and $2p\pi\Pi_+$ quasimolecular states correlated in the separated atom limit with the final state $B^{2+}(2p)+He^{+}$ (the related value of the energy is chosen as zero). The dashed curve is the initial quasimolecular state Σ_i which lies at $E=0.27$ a.u. for $R \rightarrow \infty$. The charge-exchange transitions occur primarily at the crossing of the diabatic curves $R \approx R_c = 7.4a_0$.

fixed frame where the electron wave function of the $2p$ state is not changed when the internuclear axis rotates.

In the simplest approximation the $2p\sigma$ state is populated at the well-localized regions, namely, at the moments of time when the Landau-Zener pseudocrossing ($R=R_c$) is passed. After that, the electron cloud retains its orientation in space that implies the efficient $2p\sigma\Sigma$-$2p\pi\Pi_+$ transitions in the molecular basis. Since the point $R=R_c$ is passed twice in the course of the collision, two contributions interfere. The phase difference between the amplitudes of capture at these points is the sum of the well-known Stueckelberg term and the pure geometric contribution. As a corollary of this interpretation, the orientation characteristic strongly oscillates as a function of the impact parameter ρ. The manifestation of these oscillations can be distinguished in the experimental data (Ref. [5] and private communications). The oscillations are particularly well resolved in the process similar to (1.1) but with an Ne atom instead of He [4].

However, this description appears to be incomplete. Namely, the transition between the dependence of the orientation features on the impact parameter ρ and on the scattering angle θ has not been considered carefully. (Previously, this aspect of the problem was mentioned [6] but not pursued in detail.) We demonstrate below (Secs. II and III) that, in fact, this point is necessary for the proper understanding of the interference effects observed in the charge-exchange differential cross sections for the final states with the definite electron orbital orientation. A new and appealing physical aspect of the problem is revealed (Secs. IV and V): The interference oscillations probe the repulsive region on the initial-state potential curve which lies at the internuclear separations considerably less than R_c.

II. CLASSICAL SCATTERING ANGLE IN THE CHARGE-EXCHANGE CHANNEL

We start with the analysis of the classical scattering angle in the charge-exchange channel. At first, we assume that the initial potential curve is horizontal. Both final potential curves are assumed to be degenerate and approximated by purely Coulomb repulsive interaction Z/R [$Z=2$ for the reaction (1.1)]. Actually, some splitting between $2p\sigma\Sigma$ and $2p\pi\Pi_+$ potential curves exists which is neglected below (for large R, it is related to the charge-quadrupole interaction $\sim R^{-3}$).

As discussed in the Introduction, the charge exchange occurs at the transition point $R=R_c$ on the ingoing or outgoing part of the trajectory. In this moment the Coulomb repulsion between B^{2+} and He^+ is "switched on." Considering small *laboratory* scattering angles θ (in the experiment [5], $\theta_{lab}\approx 0.1°$), one easily calculates the related angles θ_1,θ_2:

$$\theta_{1,2}=\theta_0(1\pm\sqrt{1-\rho^2/R_c^2}),\quad \theta_0=\frac{Z}{2\rho E_{lab}} \tag{2.1}$$

where E_{lab} is the collision energy. The final-state orientation parameter was previously calculated [6] taking into account the charge-exchange transitions for both passages of the point $R=R_c$ and their interference in the final p substates. The trajectory with the definite impact parameter was considered but the results were presented graphically as a function of the average scattering angle θ_0.

However, it is well known [10] that for various classical paths the interfering contributions to the final state correspond to *the same scattering angle* θ (in the channel under consideration). Hence, generally these contributions are related to the *different impact parameters* ρ. From the expressions (2.1), one can infer that the relation $\theta_1>\theta_2$ always holds (Fig. 2), i.e., the interfering trajectories do not appear.

The interference becomes possible when the short-range repulsion on the initial diabatic Σ_i potential curve is included in the calculation of the classical scattering angle in the charge-exchange channel (the curve shown in Fig. 1 was employed which accounts for the electrostatic interaction between the closed electron shells of the He and B^{3+} partners). This effect enhances $\theta_2(\rho)$ (Fig. 2), and because of it, for the given scattering angle θ, there exist such impact parameters ρ_1,ρ_2 that the relation $\theta=\theta_1(\rho_1)=\theta_2(\rho_2)$ holds. Since ρ_1 significantly exceeds ρ_2, the contributions of the classical paths to the differential cross section differ substantially due to the geometrical factor. Therefore, the interference oscillations in the differential cross section are shallower as compared with the single-trajectory (fixed-ρ) calculations.

Accounting for the short-range repulsion in the exit diabatic channel enhances $\theta_1(\rho)$, which does not lead to the appearance of the interference pattern. Quantitatively, its effect is small. Therefore, it is not included in the subsequent analysis.

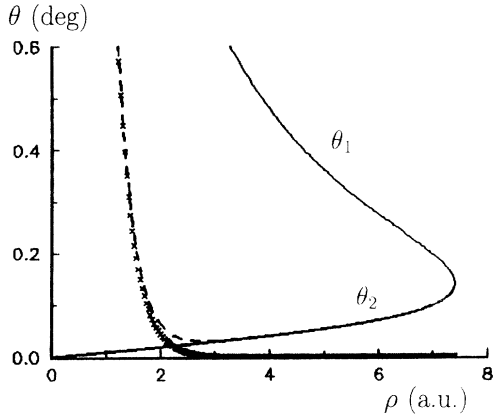

FIG. 2. The classical scattering angle θ in the laboratory frame for the charge-exchange process (1.1) as a function of the impact parameter ρ. The incident ion energy is 1.5 keV (collision velocity $v=0.07$ a.u.). The charge exchange occurs at the pseudocrossing point $R_c=7.4a_0$ on the ingoing (θ_1) or outgoing (θ_2) part of the trajectory. Solid curves, the calculations without accounting for the interaction in the initial diabatic channel; dashed curve, θ_2 calculated taking into account the short-range repulsion between B^{3+} and He; crosses, the elastic scattering.

III. FORMULATION OF THE QUANTUM THREE-STATE MODEL

We present the Hamiltonian as a sum $H=T+H_0+V+H_{\rm Cor}$, where all terms are 3×3 matrices in the minimal three-state quasimolecular basis discussed in the Introduction. For large R the basis vectors coincide with the separated atom states but with the angular momentum quantized along the internuclear axis. The nuclear kinetic-energy operator $T=-(1/2M_r)\nabla^2$ is a diagonal matrix (M_r is the reduced mass of the colliding particles). H_0 is the matrix of diabatic electronic energies,

$$H_0=\begin{bmatrix} E_i+U_i(R) & 0 & 0 \\ 0 & E_f+U_\Sigma(R) & 0 \\ 0 & 0 & E_f+U_\Pi(R) \end{bmatrix} . \quad (3.1)$$

The potential curves $U_i(R)$, $U_\Sigma(R)$, and $U_\Pi(R)$ for Σ_i, $2p\pi\Sigma$, and $2p\pi\Pi_+$ states are defined with respect to the separated atom energies E_i in the initial and E_f in the final states [i.e., $U_i(R)$, $U_\Sigma(R)$, $U_\Pi(R)\to0$ as $R\to\infty$]. Thus the potential curves shown in Fig. 1 are $E_\alpha(R)=E_\alpha+U_\alpha(R)$. The diabatic states are coupled by the nondiagonal part of the electronic Hamiltonian V and the Coriolis interaction $H_{\rm Cor}$:

$$V=\begin{bmatrix} 0 & V & 0 \\ V & 0 & 0 \\ 0 & 0 & 0 \end{bmatrix}, \quad H_{\rm Cor}=-\omega\begin{bmatrix} 0 & 0 & 0 \\ 0 & 0 & i \\ 0 & -i & 0 \end{bmatrix} , \quad (3.2)$$

where $\omega(R)=KR^{-2}M_r^{-1}$ is the angular velocity of the internuclear axis rotation for the collision with the total angular momentum K. We neglect the Coriolis coupling between Σ_i and $2p\pi\Pi_+$ states. It generates rotation-induced charge exchange which was shown to be small [6] under the conditions of the experiments [5].

As discussed in Sec. II, we use the simplest approximation for the potential curves:

$$U_i(R)=0, \quad U_\Sigma(R)=U_\Pi(R)=Z/R , \quad (3.3)$$

and later add also a short-range repulsive term (core) to the curve $U_i(R)$. The splitting of $2p\pi\Sigma$ and $2p\pi\Pi_+$ curves at large R is due to the quadrupole interaction. We neglect it here for simplicity although it could be easily incorporated in the present picture.

We have started above with the quantum-mechanical description of the relative nuclear motion in the center-of-mass system. However, in fact the angular momentum K is very large which allows us to consider K as an ordinary number and neglect the difference between the total momentum of the system (which includes the orbital momentum of the electron) and the orbital momentum of the relative nuclear motion.

Now we consider the Hamiltonian $H_1=H_0+H_{\rm Cor}$ which has the eigenvectors $|\Sigma_i\rangle, |m\rangle$. The first of them coincides with the Σ_i state introduced above and the states $|m=\pm1\rangle$ are the final atomic p substates with the orbital momentum quantized along the axis z *perpendicular* to the collision plane. This basis can be described as diabatic relative to the radial motion and adiabatic with respect to the internuclear axis rotation. It was discussed by Russek, Kimball, and Cavagnero [11]. The $m=\pm1$ eigenvalues are split by the Coriolis term $m\omega(R)$. The potential curves with inclusion of the centrifugal potential are

$$\begin{aligned} \tilde{U}_i&=E_{cm}\rho^2/R^2+U_i(R) , \\ \tilde{U}_m(R)&=(E_{cm}\rho^2+m\rho v_\infty)R^{-2}+U_\Sigma(R) . \end{aligned} \quad (3.4)$$

Here, $K=M_r v_\infty\rho$, $v_\infty=(E_{\rm lab}/2M_B)^{1/2}$ is the relative velocity of the collision, M_B is the mass of the incident (B^{3+}) ion, and $E_{\rm lab}$ is its energy. The states $|m\rangle$ are coupled with the matrix element $\pm i2^{-1/2}V$. These relations would be somewhat modified if Σ-Π splitting were taken into account.

The splitting of the potential curves $\tilde{U}_m(R)$ (3.4) for the different values of m produces the splitting of the classical turning points. In the simplified treatment [6] this splitting was not taken into account and only the phase effects were considered. This approach is reasonable when the turning point R_t for the relative radial nuclear motion lies at appreciably smaller separations than R_c. In the case of $R_t\cong R_c$ the splitting becomes important.

Under the latter conditions the position of the turning points could be effectively changed by applying the magnetic field B perpendicular to the collision plane. In this case the $m=\pm1$ potential curves $\tilde{U}_m(R)$ acquire an additional Zeeman term $mB\hat{L}_z$. Thus they become split even in the separated atom limit. Due to the large reduced mass of the nuclei, the nuclear radial wave functions are rapidly decreasing in the classically forbidden region and any slight change of the turning point position can influence significantly the final atomic state orientation. This tentative effect is analogous to that of the scanning microscope. However, it should be mentioned that our calculations for the concrete process (1.1) (described below in Sec. IV) have not demonstrated an appreciable influence of the magnetic field (with a reasonable strength) on the orientation phenomena.

Now we calculate the partial amplitudes $A_m(K)$ of the charge exchange from the initial to the final atomic p states. Since the crossing point lies at quite large internuclear separation ($R_c=7.4a$), the coupling $V(R_c)$ is small. This allows us to use the first-order diabatic perturbation theory

$$A_m(K)=\int_0^\infty \Theta_i(K,R)VQ_m(K,R)R^2dR , \quad (3.5)$$

where the wave functions in the initial (Θ_i) and final (Q) diabatic potentials are continuum states normalized by the large-R asymptotes

$$\Theta_i(K,R)\cong(2M_r/q)^{1/2}R^{-1}\sin(qR-\pi K/2+\delta_K^{(i)}) , \quad (3.6)$$

$$Q_m(K,R)\cong(2M_r/q)^{1/2}R^{-1}\sin[qR+(Z/q)\ln(2qR)-\pi K/2+\delta_K^{(m)}] \quad (3.7)$$

and $q=M_r v_\infty$ is the wave number for the relative nuclear

motion. The phase shift $\delta_K^{(i)}$ is zero when the short-range repulsion is neglected. In the present approximation the phase shifts $\delta_K^{(m)}$ coincide with the Coulomb phases and the well-known semiclassical formula [12,13] is applicable.

For the calculation of the integrals (3.5), we apply the uniform semiclassical technique by Miller [14] (see also Ref. [15]), which appears to be fairly accurate in the whole range of the parameters. We replace the coupling matrix element $V(R)$ by its value at the pseudocrossing point $V_c = V(R_c)$ (this assumption is not too restrictive and could be easily avoided). The result is as follows:

$$A_m(K) = V_c(2\pi M_r |F_m^{(m)} - F_i^{(m)}|^{-1} x_m^{1/2} p_m^{-1})^{1/2} \mathrm{Ai}(x_m) , \tag{3.8}$$

where

$$x_m = [\tfrac{3}{2} S_m(R_m)]^{2/3} , \tag{3.9}$$

$$S_m(R) = \int_{R_{ti}}^{R} p_i(R')dR' - \int_{R_{tm}}^{R} p_m(R')dR' , \tag{3.10}$$

$$p_i(R) = \{2M_r[E_{cm} - \tilde{U}_i(R)]\}^{1/2} ,$$

$$p_m(R) = \{2M_r[E_{cm} - \tilde{U}_m(R)]\}^{1/2} .$$

Here, R_m are the transition points defined as solutions of the equation $p_i(R_m) = p_m(R_m)$,

$$F_\alpha^{(m)} = \left. \frac{d\tilde{U}_\alpha(R)}{dR} \right|_{R=R_m} ,$$

R_{ti} and R_{tm} are the turning points for the potentials (3.4), and $\mathrm{Ai}(x)$ is the Airy function. One can see that in the classically allowed region the expression (3.8) merges with the Landau-Zener formula, but with the Stueckelberg oscillations included, as it was described by Landau [12,16]. Equation (3.8) is uniformly applicable also in the case when the transition points R_m are close to the turning points.

The next step is summation of the partial-wave expansion. We are interested in the small scattering angles θ, i.e., the large angular momenta K are involved. Hence, the summation can be replaced by the integration and the well-known approximation of the Legendre polynomials via the Bessel function,

$$P_K(\cos\theta) \cong J_0((2K+1)\sin\tfrac{1}{2}\theta) , \tag{3.11}$$

can be employed. This leads to the eikonal-type formula for the angular-dependent charge-exchange amplitudes $f_m(\theta)$:

$$f_m(\theta) = \frac{1}{2M_r^2 v_\infty^2} \int_0^\infty \exp(iK\pi/2) J_0(2K \sin(\theta/2)) \times A_m(K) \exp(i\delta_K^{(i)})(2K+1)dK . \tag{3.12}$$

The applicability of the conventional stationary phase integration procedure [12] in the present case may be questionable, since the small scattering angle phenomena are considered. Therefore, below we prefer a purely numerical computation. The importance of the Bessel transforms for the calculation of the orientation-type parameters was stressed previously by Shakeshaft and Macek [17].

IV. RESULTS OF CALCULATIONS

The results of our calculations for the amplitudes A_m with the formula (3.8) are shown in Fig. 3 in comparison with the amplitudes calculated with the formulas from Ref. [6]. For the sake of graphical convenience, the reduced amplitudes B_m are presented. They are defined as

$$B_m = A_m V_c^{-1} (2\pi M |F_m^{(m)} - F_A^{(m)}|^{-1} x_m^{1/2} p_m^{-1})^{-1/2} . \tag{4.1}$$

Both approximations give close results and the difference appears for $\rho \simeq R_c$. In the classical description of the nuclei motion [6], the curves $B_m(\rho)$ have an abrupt cutoff exactly at $\rho = R_c$. In the semiclassical approximation the cutoff is replaced by the cusp in $B_m(\rho)$. These cusps are

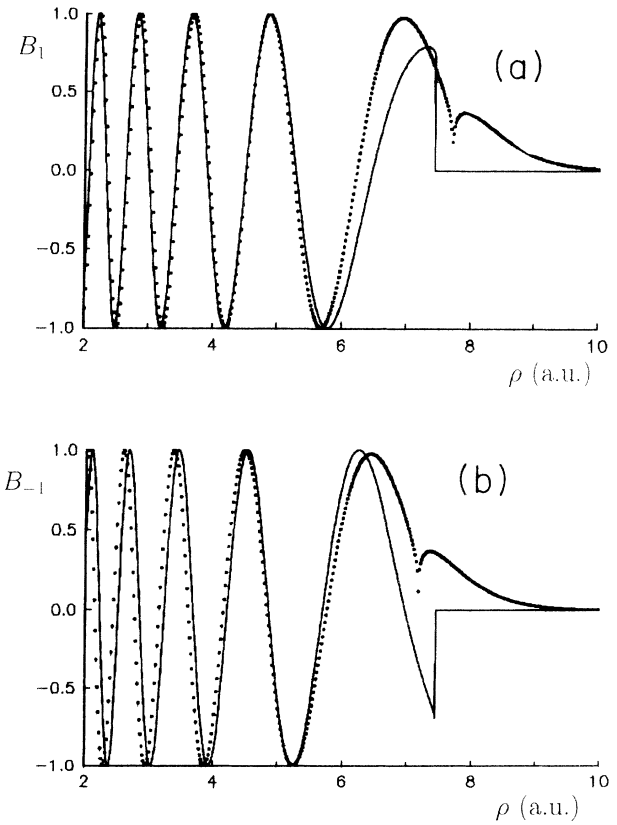

FIG. 3. The reduced amplitudes B_m (4.1) as a function of the impact parameter ρ for the charge exchange (1.1) into the final $B^{2+}(2p)$ states with a definite projection m of the angular momentum on the axis normal to the collision plane ($v = 0.07$ a.u.): (a) $-m = 1$, (b) $-m = -1$. Dots present semiclassical calculations; solid lines, classical theory [6]. In the state with $m = 1$ the electron rotates around the nucleus in the same sense as the incident ion (the preferential population of this state is in agreement with the so-called velocity matching arguments).

artificial since their appearance is specifically related to the last factor in (4.1) [note that the amplitudes $A^{(m)}(\rho)$ given by Eq. (3.8) do not have any peculiarity at this point]. Positions of the cusp (i.e., boundaries of the regions of classically allowed population) somewhat differ for $m=1$ and -1, reflecting the role of the Coriolis interaction. In the other terms it could be said that this is a manifestation of the splitting of the pseudocrossing points R_m (see Sec. III) by the Coriolis interaction [11].

The oscillatory behavior of the amplitudes A_1 and A_{-1} is interpreted as a result of the interference between the contributions of the two passages of the pseudocrossing point R_c (see the Introduction). The oscillations in A_1 and A_{-1} differ in phase which implies the final-state orientation (i.e., the difference between $|A_1|$ and $|A_{-1}|$). Now we consider the related phases in somewhat more detail.

The second phase integral entering the expression (3.10) for the phase $S_m(R)$ can be recast in the form

$$\int_{R_{tm}}^{R}\{2M_r[E_{cm}-\tilde{U}_m(R)]\}^{1/2}dR \cong \int_{R_{t0}}^{R}\{2M_r[E_{cm}-\tilde{U}_0(R)]\}^{1/2}dR + m\int_{R_{t0}}^{R}\omega(R)\{2[E_{cm}-\tilde{U}_0(R)]/M_r\}^{-1/2}dR\ , \tag{4.2}$$

where $\tilde{U}_0(R)$ is the final-state potential curve with inclusion of the centrifugal potential but without the Coriolis term [cf. (3.4)]:

$$\tilde{U}_0(R)=E_{cm}\rho^2/R^2+U_\Sigma(R) \tag{4.3}$$

and R_{t0} is the related turning point. The last term in the right-hand side of Eq. (3.2) appears due to the Coriolis contribution in $\tilde{U}_m(R)$ and has an evident geometrical interpretation as an angle of rotation of the internuclear axis in the course of the collision when the separation of the nuclei varies from R_{t0} to R.

Thus, in agreement with the result obtained previously [6], the interference phase $S_m(R_m)$ is a sum of the conventional Stueckelberg term and of the purely geometric contribution equal to the angle β (see [6]).

However, generally, the probabilities depending on the impact parameter should be considered as an intermediate theoretical result; only the angular distributions are directly observable. Transition to the angular dependencies according to Eq. (3.12) could introduce some additional interference phenomena with the phases of the same order as these discussed above. In the present context the important role is played by the elastic-scattering phase $\delta_K^{(i)}$ for the initial diabatic channel. As indicated above, it is nonzero due to the effect of the short-range repulsion. The phase was calculated numerically employing the potential curves shown in Fig. 1.

The integrand in (3.12) has quite complicated dependence on K (or ρ). In Fig. 4 we show the amplitude $A_{-1}(K)$ (dotted line) and the factor $A_{-1}(K)\cos(\delta_K^{(i)})$ (solid line) which enter the integrand beside the Bessel function J_0. The amplitude $A_{-1}(K)$ exhibits the conventional Airy-type oscillatory pattern. The factor

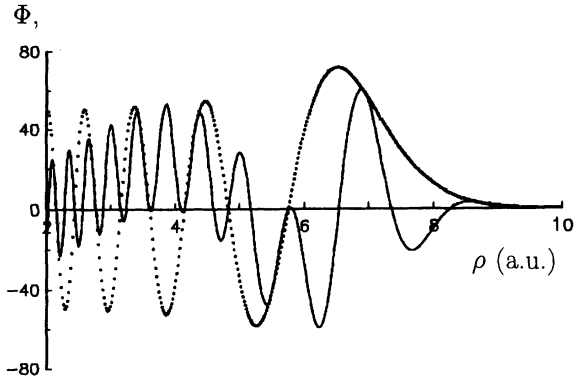

FIG. 4. The factor $\Phi(\rho)$ entering the integrand in (3.12): dotted line, $\Phi=A_{-1}(K)$; solid line, $\Phi=A_{-1}(K)\cos(\delta_K^{(i)})$. The structure of this factor is important for the transition from the impact-parameter-dependent to the angular-dependent amplitudes of the charge-exchange process (see discussion in the text).

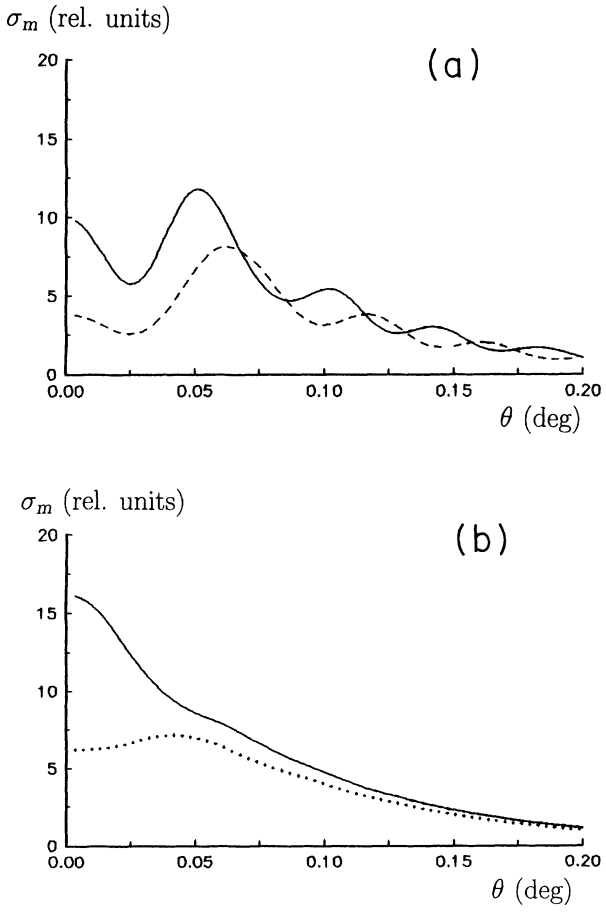

FIG. 5. The cross sections σ_m for the charge exchange (1.1) into the final states with the definite electron angular momentum projection m (solid line, $m=1$; dashed line, $m=-1$): (a) present semiclassical calculations taking into account the repulsive core in the initial diabatic channel; (b) the same as (a) with the repulsive core omitted.

$A_{-1}(K)\cos(\delta_K^{(i)})$ due to the influence of the scattering phase $\delta_K^{(i)}$ in the incident diabatic channel manifests the more complicated structure: Now the low-frequency Airy-type oscillations are superimposed by the high-frequency oscillations generated by the $\cos(\delta_K^{(i)})$ factor. Generally, the stationary-phase arguments show that in calculations of the integral (3.12), the lower-frequency contribution influences the scattering on the larger angles. However, as discussed in the end of Sec. III, we avoid the stationary-phase integration procedure and present the results of the numerical calculations.

The cross sections σ_m of the charge exchange into the final states with the definite m are shown in Fig. 5. Without inclusion of the repulsive interaction in the incident channel [Fig. 5(b)], the final-state orientation (defined as the ratio $[\sigma_1(\theta)-\sigma_{-1}(\theta)]/[\sigma_1(\theta)+\sigma_{-1}(\theta)]$) is a monotonously decreasing function of the scattering angle θ. In agreement with the preceding discussion, the oscillations appear only when the repulsive core is included in the calculations [Fig. 5(a)]. The general cross-section pattern is close to that observed in the experiments [5]; the detailed comparison requires folding of the theoretical data with the experimental uncertainties and will be carried out separately.

V. CONCLUSION

In conclusion it is worthwhile to stress that the present study is a model one. Its object is analysis of the physical picture, whereas the results with the higher numerical precision are obtainable in the large-scale close-coupling calculations [18]. We choose the minimal basis of physically relevant states and do not include the near-lying $2s$ state of the ion B^{2+} which gives the major contribution to the integral charge-exchange cross section. The other simplifying assumption is the use of the perturbation theory in the calculation of the transition amplitudes. The more accurate potential curves also could be used.

However, all these approximations do not influence the principle qualitative conclusion of our study: The interference oscillations in the asymmetry parameter probe the inner repulsive region of the initial-state potential curve which lies at the internuclear separations significantly less than the transition point R_c.

ACKNOWLEDGMENTS

We gratefully acknowledge very stimulating discussions with P. Roncin. The hospitality of the Laboratoire des Collisions Atomiques et Moleculaires (Université Paris–Sud, Orsay) is highly appreciated. The work was completed during the visit of one of the authors (V.N.O.) to the University of Bielefeld supported by the Deutsche Forschungsgemeinschaft in Sonderforschungbereich 216 "Polarisation und Korrelation in atomaren Stoßprozessen."

[1] N. Andersen, J. W. Gallagher, and I. V. Hertel, Phys. Rep. **165**, 1 (1988).
[2] E. E. B. Campbell, H. Schmidt, and I. V. Hertel, Adv. Chem. Phys. **72**, 37 (1988).
[3] D. Dowek, J. C. Houver, and C. Richter, in *Invited Papers of the XVII International Conference on the Physics of Electronic and Atomic Collisions,* edited by W. R. MacGillivray, I. E. McCarthy, and M. C. Standage (Adam Hilger, London, 1991), p. 537.
[4] J. P. Hansen, N. Andersen, A. Dubois, S. E. Nielsen, C. Adjouri, M. Barat, M. L. Gaboriaud, V. Ostrovsky, and P. Roncin, in *Correlations and Polarization in Electronic and Atomic Collisions and (e,2e) Reactions,* edited by P. J. O. Teubner and E. Weigold, IOP Conference Series No. 122 (Institute of Physics, Bristol, 1991), p. 307.
[5] P. Roncin, C. Adjouri, M. N. Gaboriaud, L. Guillemot, M. Barat, and N. Andersen, Phys. Rev. Lett. **65**, 3261 (1990).
[6] V. N. Ostrovsky, J. Phys. B **24**, L507 (1991).
[7] V. N. Ostrovsky, J. Phys. B **24**, 4553 (1991).
[8] D. H. Jaecks, F. J. Ericksen, W. de Rijk, and J. Macek, Phys. Rev. Lett. **35**, 723 (1975).
[9] F. J. Eriksen, D. H. Jaecks, W. de Rijk, and J. Macek, Phys. Rev. A **14**, 119 (1976).
[10] E. E. Nikitin and S. Ya. Umanskii, *Theory of Slow Atomic Collisions* (Springer, Berlin, 1984).
[11] A. Russek, D. B. Kimball, and M. J. Cavagnero, Phys. Rev. A **23**, 139 (1981).
[12] L. D. Landau and E. M. Lifshits, *Quantum Mechanics* (Pergamon, Oxford, 1965).
[13] S. Flugge, *Practical Quantum Mechanics* (Springer, Berlin, 1971).
[14] W. H. Miller, J. Chem. Phys. **48**, 464 (1968).
[15] M. S. Child, *Molecular Collision Theory* (Academic, London, 1974).
[16] L. D. Landau, Phys. Z. Sowjetunion **1**, 88 (1932).
[17] R. Shakeshaft and J. Macek, Phys. Rev. A **6**, 1876 (1972); **7**, 1554 (1973).
[18] J. P. Hansen, L. Kocbach, A. Dubois, and S. E. Nielsen, Phys. Rev. Lett. **64**, 2491 (1990).